Finite-Element Modeling of 3C-SiC Membranes

R. G. DeAnna*, J. Mitchell**, C. A. Zorman**, and M. Mehregany**
*US Army Research Laboratory, NASA Glenn Research Center, Cleveland, OH, USA,
torgd@grc.nasa.gov
**Case Western Reserve University, Cleveland, OH, USA

ABSTRACT

Finite-element modeling (FEM) of 3C-SiC thin-film membranes on Si substrates was used to determine the residual stress and center deflection with applied pressure. The anisotropic, three-dimensional model includes the entire 3C-SiC membrane and Si substrate with appropriate material properties and boundary conditions. Residual stress due to the thermal-expansion-coefficient mismatch between the 3C-SiC film and Si substrate was included in the model. Both before- and after-etching, residual stresses were calculated. In-plane membrane stress and normal deflection with applied pressure were also calculated. FEM results predict a tensile residual stress of 259 MPa in the 3C-SiC membrane before etching. This decreases to 247 MPa after etching the substrate below the membrane. The residual stress experimentally measured on samples made at Case Western Reserve University was 280 MPa on post-etched membranes. This is excellent agreement when an additional 30-40 MPa of residual stress to account for lattice mismatch is added to the FEM results.

Keywords: Silicon Carbide, MEMS, ANSYS, membrane, FEM.

1. INTRODUCTION

3C-SiC is an important semiconductor material for high-temperature, harsh-environment applications. 3C-SiC has better mechanical and electrical properties at high temperature than Si. 3C-SiC is also chemically inert and can be used in corrosive and other chemically-harsh environments.

The load-deflection test has been used to determine material properties like Young's modulus and Poisson's ratio for a variety of materials. The test uses a membrane loaded with an applied pressure. An interferometer or other device is then used to accurately measure the center deflection of the membrane as a function of applied pressure. The pressure versus deflection for a square membrane is governed by [1]

$$P = \frac{3.41h}{a^2}\sigma_o w_o + \frac{1.33f(\nu)h}{a^4}\frac{E}{1-\nu}w_o^3 \quad (1)$$

where P is an applied pressure, w_0 is the membrane center deflection, h is the thickness, $2a$ is the width, ν is Poisson's ratio, σ_o is residual stress, and $f(\nu)= 1.446-0.427\nu$ is an empirically derived expression. The resulting graph of pressure versus deflection can then be fitted to the governing equation, and residual stress and Young's modulus extracted. The residual stress is obtained from the low-deflection region of the curve where the first term dominates in equation 1; Young's modulus is obtained from the large-deflection region where the residual-stress term is small compared to the stress due to the applied pressure.

Residual stress in 3C-SiC thin films grown on a Si substrate is due to two effects: a lattice mismatch between the 3C-SiC and Si single crystals, and a thermal component due to the different thermal coefficients of expansion. The SiC-Si lattice-mismatch component is typically 30-40 MPa [2]; the thermal component is usually dominant for films at typical growth temperatures around 1600 K [3]. 1600 K was the growth temperature for our membrane films.

2. FINITE-ELEMENT MODEL GEOMETRY AND MESH

The Young's modulus extracted from the experimental load-deflection test is input to the finite-element model. The load-deflection test gives the in-plane Young's modulus. The out-of-plane value is calculated as 0.66 times the in-plane value [4]. The FEM predicts the residual stress, which is then compared with the experimental value. The model incorporates both the 3C-SiC film and the Si substrate and mimics the complete fabrication process from 3C-SiC film growth at high temperature, cooling to room temperature, and etching the Si substrate beneath the membrane. For this study, 1-mm square 3C-SiC membranes were fabricated on a 4-inch diameter wafer. These films were grown on a (100) Si substrate in a cold-wall, vertical-geometry, RF-induction-heated APCVD (Atmospheric Pressure Chemical Vapor Deposition) reactor.

The geometry of the die is shown in Figure 1. It contains a 2-mm square die with a 1-mm square by 2 μm-thick 3C-SiC membrane on a 500-μm thick Si substrate. 3C-SiC membranes were bulk micromachined from the Si substrates using standard KOH-based wet anisotropic etching techniques.

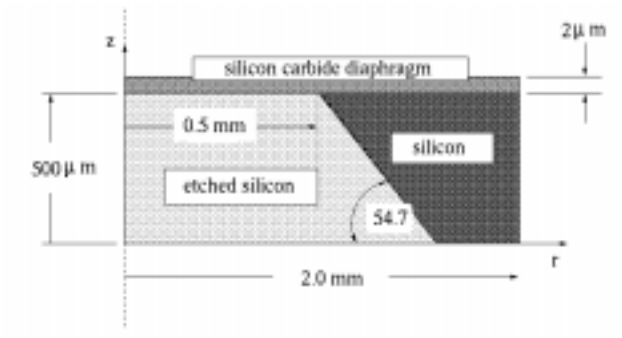

Figure 1: Cross-sectional geometry of pre- and post-etch die with 3C-SiC membrane.

Quarter symmetry is used in the FEM. The model uses 8-node brick elements for the Si substrate and 4-node shell elements for the 3C-SiC film and membrane. Figure 2 shows a top view of the FEM grid with a standard mesh.

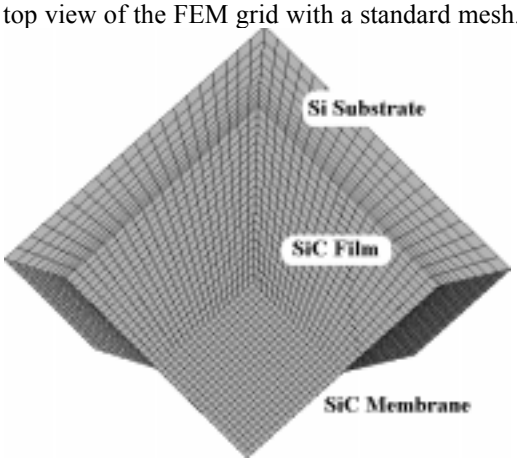

Figure 2: Top view of grid with standard mesh.

The standard mesh contains 20x20 shell elements in the membrane and a pair of 20x20 shell element meshes for the 3C-SiC film outside the membrane. Uniform grid spacing is used. A pair of 20x20x12, brick-element meshes represent that part of the Si substrate not etched. Another 20x20x12, brick-element mesh represents the etched region of the Si substrate under the membrane. Since the 3C-SiC layer is much thinner than the Si substrate, the mesh was stretched in the z direction to allow thinner elements near the 3C-SiC film. The standard-mesh results were verified using a finer mesh as shown in Figure 3. The fine mesh contains 40x20 shell elements in the membrane. The elements are square at the center of the membrane and narrow near the substrate. The mesh is also stretched so as to create smaller elements in regions of high gradients at the corners of the membrane.

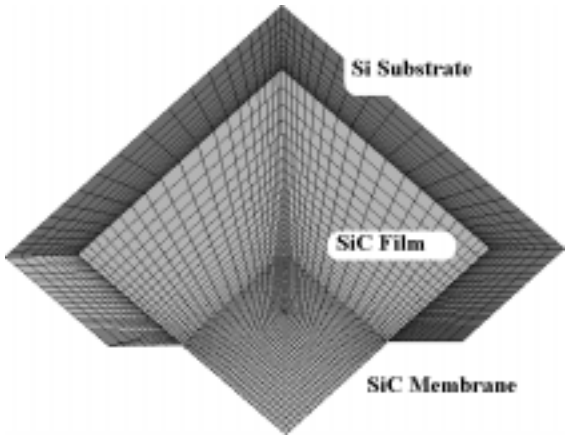

Figure 3: Top view of grid with fine mesh.

Figures 2 and 3 show the after-etched, top-view FEM. The before-etch, side-view model shown in Figure 4 includes the Si elements in the substrate region below the membrane. The mesh after etching is shown in Figure 5.

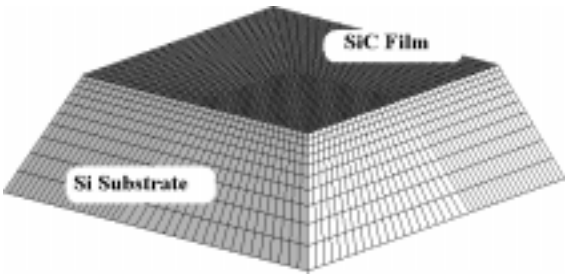

Figure 4: Side view of standard grid before etching.

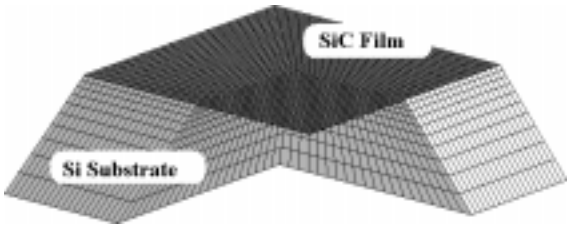

Figure 5: Side view of standard grid after etching.

The outside of the mesh gets wider at the bottom to account for the anisotropic Si wet etch. A mesh with vertical outside edges would create poorly-shaped elements at the bottom of the substrate. Symmetry boundary conditions were applied on the symmetry planes. The vertical displacement was fixed at a single point. These boundary conditions allow mesh curvature and thermal shrinkage and induce no artificial stress.

3. FINITE-ELEMENT MODEL PROCEDURE

The ANSYS® [5] finite-element package was used to model the two-step fabrication process: cooling from film growth to room temperature and wet etching the substrate region to create the membrane. The two steps allow calculation of before- and after-etch residual stress. All the

elements were included during the cooling step; the etched elements in the substrate were then removed to calculate the after-etch state. The pressure was applied in the third step. A non-linear FEM was used because the membrane displacements are a large fraction of the membrane thickness for the applied pressures under consideration. Furthermore, residual stress acts in the plane of the membrane and would not affect the out-of-plane loads in a simple linear analysis.

The thermal residual stress is caused by a thermal-expansion-coefficient mismatch between the 3C-SiC film and Si substrate. A plot of thermal-expansion coefficients versus temperature for 3C-SiC [6] and Si [7] is given in Figure 6. 3C-SiC has a larger coefficient above 400 K. The residual stress is proportional to the area between the curves between growth and room temperature.

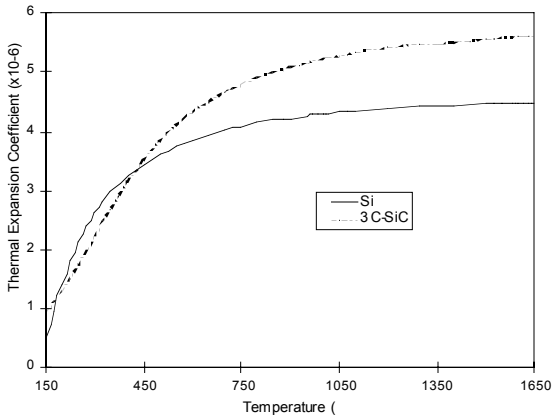

Figure 6: Thermal expansion coefficients for Si and 3C-SiC versus temperature.

4. FINITE-ELEMENT MODEL RESULTS

A single case was studied with membrane thickness h of 1.48 μm, side length a of 1 mm, and measured in-plane [(100) plane] Young's modulus of 415 GPa. A Poison's ratio of 0.23 was used. With an applied pressure of 370 kPa, the experimentally-measured center deflection, w_0, was 22.4 μm. The isotropic FEM center deflection was 21.0 μm using the standard grid and 20.9 μm with the fine grid. The similarity of these FEM values shows that the standard grid is suitable. Note that the center deflection is more than a factor of ten greater than the membrane thickness. This is clearly in the non-linear regime. The after-etching, measured residual stress, which includes the 30-40 MPa stress due to lattice mismatch, was 280 MPa; the FEM residual stress was 259 MPa before etching and 247 MPa after etching. The experimental and FEM results are summarized in Table 1. Included in Table 1 are the center-deflection results for pressure applied from the bottom (inside the mesh). Note that the FEM does not include lattice-mismatch residual stress. Adding 30 to 40 MPa more residual stress to the FEM value brings it close to the measured datum.

Step	Pre-etch No Pressure		Post-etch No Pressure		Post-etch Pressure	
Result	Exp.	FEM	Exp.	FEM	Exp.	FEM
w_0 (μm)	-	-.4	-	-.45	22.4	21.0
σ_0 (MPa)	-	259	280	247	-	479

Table 1. Pre- and post-etch center deflection and stress for the experiment and FEM.

Figure 7 presents the FEM non-dimensional deflection versus distance from the center of the membrane to the edge of the mesh for a pressure of 370 kPa. The curve has been non-dimensionalized using $/a$, where a is the membrane side length, and $_0 = 12w_0/h$.

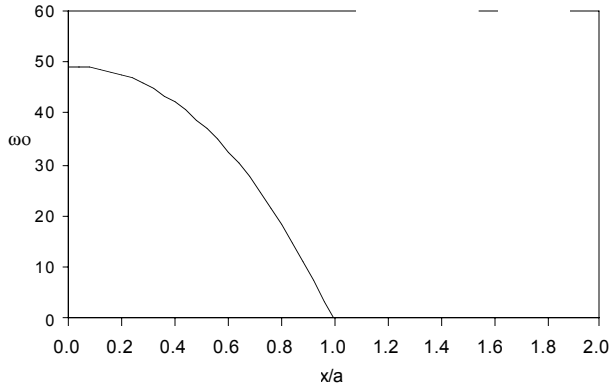

Figure 7. Non-dimensional membrane deflection with pressure versus normalized distance from the membrane center to the edge of the mesh for the FEM.

Figure 8 shows the FEM before- and after-etch curves of the membrane residual stress and stress with applied pressure. The radial stress component is plotted. The stress has been non-dimensionalized using $\sigma = \sigma_{xx} a^2 / D$, where $D = Eh^3/12(1-\nu^2)$ denotes the flexural rigidity. Upon etching, the residual stress decreases slightly in the membrane region and increases slightly outside the membrane. The maximum stress for the case with applied pressure was 467 MPa. As shown, the stress is nearly constant from the center of the membrane out to the edge.

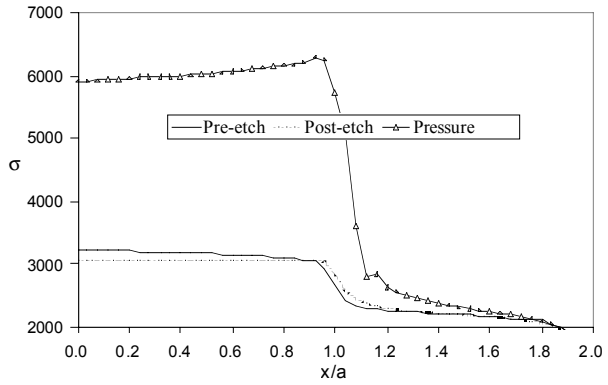

Figure 8: Normalized stress distribution from membrane center to the edge of the mesh for pre-etch, post-etch, and applied pressure for the FEM.

This shape is unlike that predicted by small-deflection-theory where the maximum stress is at the membrane edge. Although not shown, the stress in the membranes was primarily the in-plane component. The stress normal to the plane was several orders-of-magnitude less than the in-plane value. At these large deflections, the load-deflection technique essentially measures the in-plane Young's modulus. The membrane is stretching like a balloon.

5. CONCLUSION

The load-deflection experiment is used to measure both residual stress and Young's modulus. The residual-stress measured by this technique includes both the stress due to lattice mismatch and that due to thermal expansion mismatch. The FEM residual stress agrees with the experimental value when 30-40 MPa more stress is added to account for the lattice-mismatch component. The FEM maximum deflection with applied pressure is just slightly less than the experiment. According to the FEM, the residual stress in the membrane decreases from 259 MPa before etching to 247 MPa after etching, or 4.6 percent. The residual stress outside the membrane increases slightly after etching. In essence, etching relaxes the residual strain energy in the membrane and shifts it to the region outside the membrane. The results also show that the residual stress inherent in the film before etching is approximately 4-5% greater than the after-etched value measured by the load-deflection technique. These results are important since the load-deflection technique only determines after-etch residual stress, while material scientists desire to know the residual stress inherent in the film. Although not shown, the FEM results with applied pressure show that in-plane membrane stress is several orders-of-magnitude larger than the stress normal to the membrane. Thus, the load-deflection technique is measuring the bi-axial or in-plane residual stress at these high deflections.

ACKNOWLEDGEMENTS

The work at CWRU was supported by the Army Research Office under a Multidisciplinary Research Initiative, Contract No. DAAH04-95-10097.

REFERENCES

[1] J.Y. Pan, P. Lin, F. Maseeh, and S. D. Senturia, "Verification of FEM analysis of load-deflection methods for measuring mechanical properties of thin films," in Tech. Dig. IEEE Solid-State Sensors and Actuator Workshop, Hilton Head, SC, 70-73, 1990.

[2] L.Tong and M. Mehregany, "Mechanical Properties of 3C Silicon Carbide," Appl. Phys. Lett. 60 (24), 2992-2994, 1992.

[3] C.M.Su, A. Fekade, M. Spencer, and M. Wuttig, "Stresses in chemical vapor deposited epitaxial 3C-SiC membranes," J. Appl. Phys. 77 (3), 1280-1283, 1995.

[4] Z.C. Feng, W.J. Choyke, and J.A. Powell, "Raman determination of layer stresses and strains for heterostructures and its application to the cubic SiC/Si system," J. Appl. Phys. 64 (12), 6827-6835, 1988.

[5] ANSYS, Inc., Southpointe, 275 Technology Drive, Canonsburg, PA 15317.

[6] R.R. Reeber and K. Wang, "Thermal expansion and lattice parameters of group IV semiconductors," Mat. Chem. and Phys. 46, 259-264,1996.

[7] R.R. Reeber and K. Wang, "Thermal Expansion of β-SiC, GaP and InP," Mat. Res. Soc. Symp. Proc. 410, 211-216, 1996.